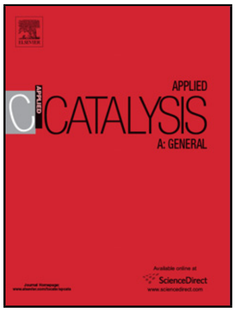

Title: EFFICIENT CYCLOHEXANE OXIDATION WITH HYDROGEN PEROXIDE CATALYSED BY A C-SCORPIONATE IRON(II) COMPLEX IMMOBILIZED ON DESILICATED MOR ZEOLITE

Author: L.M.D.R.S. Martins A. Martins E.C.B.A. Alegria A.P. Carvalho A.J.L. Pombeiro

PII:	S0926-860X(13)00303-7
DOI:	http://dx.doi.org/doi:10.1016/j.apcata.2013.05.022
Reference:	APCATA 14234
To appear in:	*Applied Catalysis A: General*
Received date:	27-2-2013
Revised date:	15-5-2013
Accepted date:	18-5-2013

Please cite this article as: L.M.D.R.S. Martins, A. Martins, E.C.B.A. Alegria, A.P. Carvalho, A.J.L. Pombeiro, EFFICIENT CYCLOHEXANE OXIDATION WITH HYDROGEN PEROXIDE CATALYSED BY A C-SCORPIONATE IRON(II) COMPLEX IMMOBILIZED ON DESILICATED MOR ZEOLITE, *Applied Catalysis A, General* (2013), http://dx.doi.org/10.1016/j.apcata.2013.05.022

*Graphical Abstract (for review)

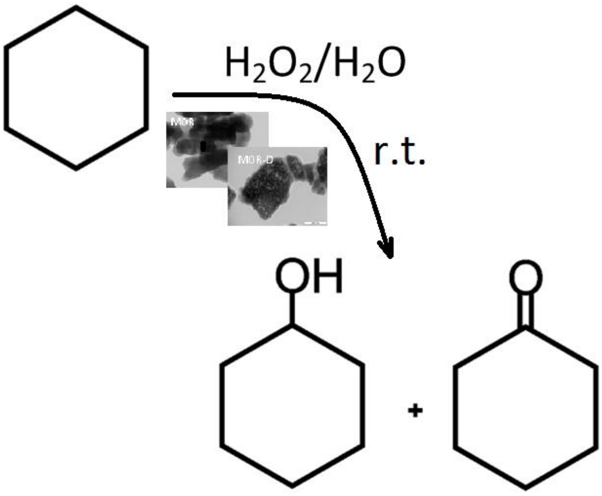

- The C-scorpionate Fe(II) complex is suitably supported on desilicated MOR zeolite
- Generation of mesoporosity in commercial MOR improves the anchorage of Fe complex
- The heterogeneous Fe system is notably efficient for the oxidation of cyclohexane
- The catalytic activity of the Fe complex is highly improved by heterogenization

EFFICIENT CYCLOHEXANE OXIDATION WITH HYDROGEN PEROXIDE CATALYSED BY A C-SCORPIONATE IRON(II) COMPLEX IMMOBILIZED ON DESILICATED MOR ZEOLITE

L.M.D.R.S. Martins[a,b,]*, A. Martins[a,c], E.C.B.A. Alegria[a,b], A.P. Carvalho[d], A.J.L. Pombeiro[b]

[a]*Área Departamental de Engenharia Química, Instituto Superior de Engenharia de Lisboa, Rua Conselheiro Emídio Navarro, 1, 1959-007 Lisboa, Portugal. e-mail: lmartins@deq.isel.ipl.pt, Telephone: +351 218317163, Fax: +351 218317267.*

[b]*CQE, Complexo I, Instituto Superior Técnico, Technical University of Lisbon, Av. Rovisco Pais, 1049-001 Lisboa, Portugal*

[c]*CIEQB, Instituto Superior de Engenharia de Lisboa, Rua Conselheiro Emídio Navarro, 1 1959-007 Lisboa, Portugal.*

[d]*Departamento de Química e Bioquímica and CQB, Faculdade de Ciências, Universidade de Lisboa, Campo Grande Ed. C8, 1749-016 Lisboa, Portugal*

Abstract

The hydrotris(pyrazol-1-yl)methane iron(II) complex $[FeCl_2\{\eta^3\text{-}HC(pz)_3\}]$ (**Fe**, pz = pyrazol-1-yl) immobilized on commercial (MOR) or desilicated (MOR-D) zeolite, catalyses the oxidation of cyclohexane with hydrogen peroxide to cyclohexanol and cyclohexanone, under mild conditions. MOR-D/**Fe** (desilicated zeolite supported [$FeCl_2\{\eta^3$-$HC(pz)_3\}$] complex) provides an outstanding catalytic activity (TON up to 2.90 x 10^3) with the concomitant overall yield of 38%, and can be easy recovered and reused.

The MOR or MOR-D supported hydrotris(pyrazol-1-yl)methane iron(II) complex (MOR-**Fe** and MOR-D/**Fe**, respectively) were characterized by X-ray powder diffraction, ICP-AES, and TEM studies as well as by IR spectroscopy and N_2 adsorption at -196 ºC. The catalytic operational conditions (*e.g.*, reaction time, type and amount of oxidant, presence of acid and type of solvent) were optimized.

Keywords: C-scorpionates, iron(II), cyclohexane oxidation, supported catalysis, desilicated MOR zeolite

1. Introduction

The current interest in tris(pyrazolyl)methanes *e.g.*, $HC(pz)_3$ (Tpm, pz = pyrazol-1-yl) arises from their diverse applications [1]. Of particular synthetic interest is the use of transition metal complexes bearing such ligands in oxidation catalysis, namely toward organic synthesis. In fact, some of us have demonstrated [2] that several tris(pyrazol-1-yl)methane complexes can act, in homogeneous media, as catalysts or catalyst precursors for relevant alkane oxidation reactions, namely peroxidative oxygenations (to give alcohols and ketones) and carboxylations (to produce carboxylic acids), a field that remains rather unexplored due to the difficulty of the activation of the C-H and C-C bonds in such unreactive compounds that prevents their broad usage for the direct syntheses of added value chemical products [3]. An example with industrial significance concerns the oxidation of cyclohexane to cyclohexanol and cyclohexanone that are important reagents for the production of adipic acid and caprolactam used for the manufacture of nylon. The industrial process uses a homogeneous cobalt species as catalyst and dioxygen as oxidant, at a considerably high temperature (150 ºC), forming the oxidation products in a low yield to achieve a good selectivity [3g-i] and so the need to search for more active systems under milder reaction conditions has been recognized [3g-i,4].

The immobilization of a catalyst or a catalyst precursor complex on a solid support is a common and suitable procedure to combining the advantages of homogeneous and heterogeneous catalyses. In fact, the heterogeneization of homogeneous catalysts has become an important strategy to obtain supported catalysts that retain the homogeneous catalytic sites, with the advantages of easy separation and recycling [5,6]. The mechanical stability and high porosity of zeolites could be advantageous during catalysts recycling and reuse procedures. Nevertheless, the purely microporous character of zeolites can be a drawback for processing large molecules of nanometer scale sizes, since it imposes diffusion limitations due to the restricted access of those molecules to the porous structure. This is the main reason why zeolites are not widely used as supports for large active species, when compared with mesoporous solids. In fact, due to the microporous nature, the immobilization is typically confined to the external surface resulting in limiting uptake and protection of the guest molecule [7]. In this sense, the use of zeolites with hierarchical porosity, combining micro and mesoporosity, can efficiently combine the properties inherent to zeolites with the presence of mesopores. The desilication, a post-synthesis [8] controlled extraction of silicon from the zeolite framework in alkaline medium, results on the generation of mesoporosity in zeolite crystals, and also on the enlargement of the existent micropores which can be translated in a certain hierarchical porous structure. In the last years, the volume of publications concerning the characterization and potential applications of desilicated zeolites is increasing, especially focusing MFI zeolite [9,10] but also other structures like BEA [11], FER [12] and MOR [9,13,14]. Although the first explored applications are in the domain of heterogeneous catalysis, recent publications have been showing more potentialities for desilicated zeolites as adsorbents [15] or enzyme carriers [16]. However, the application of hierarchical zeolites as hosts for transition metal complexes is scarcely reported: Guo and Kim [17] reported the immobilization of a salen Ti complex on MFI with mesoporosity and achieved high activity and stability in the epoxidation of (-)-α-pinene with H_2O_2; Jin *et al.* [18] described the effect of the immobilization of palladium acetate in thin ionic liquid layers on mesopore walls of hierarchical MFI zeolite and found improved catalytic activity and high stability for the Suzuki reaction.

Mordenite (MOR) is a member of the large pore zeolite family. It consists of a 12-membered ring (MR) system of pore channels of 0.67 × 0.70 nm interconnected by 8-MR pores of 0.34 × 0.48 nm. Since this zeolite has excellent thermal and mechanic stability it is one of the most used zeolites in industrial applications, especially as heterogeneous catalysts in processes such as alkylation [19] and short-chain paraffin hydroisomerization

[20]. The desilication conditions for this structure were already studied and optimized by some of us [9].

In the present study, we aim to explore the ability of desilicated MOR zeolite (MOR-D) as a support for the immobilization of tris(pyrazol-1-yl)methane-type scorpionate complexes and evaluate the catalytic potential of the heterogeneized species for the peroxidative oxidation of cyclohexane to the cyclohexanol and cyclohexanone mixture under mild conditions, namely concerning the possibility of recycling.

2. Experimental

2.1. Catalyst and support preparation

The hydrotris(pyrazol-1-yl)methane [$HC(pz)_3$, Tpm, pz = pyrazol-1-yl] [21], as well as the iron complex [$FeCl_2\{\eta^3\text{-}HC(pz)_3\}$] (**Fe**, Figure 1) [2f], were prepared according to published procedures, (the complex) under an atmosphere of dinitrogen (Air Liquid Portugal) using standard vacuum and inert-gas flow techniques. The solvents were purified by standard procedures and freshly distilled immediately prior to use.

The parent material used as support was a mordenite structure (MOR) in ammonium form, supplied by Zeolyst (CBV21A; lot 2200-83), that according with the technical report has a SiO_2/Al_2O_3 = 20. The alkaline treatment was performed using NaOH (Merk p.a.) solution as desilicating agent, following the procedure previously published [9]. Briefly, the zeolite was stirred with 0.5 M NaOH solution using a proportion of 330 mg/10 mL solution. After the treatment, the zeolite suspension was filtered off, washed thoroughly up to pH 7 and then dried overnight at 90 ºC.

2.2. Immobilization of the iron complex $[FeCl_2\{\eta^3\text{-}HC(pz)_3\}]$

For the immobilization of **Fe** in MOR and MOR-D the wet-impregnation method was used following the procedure previously reported by some of us [1h]. The iron complex (10 mg) was dissolved in methanol (5 mL, Lab-Scan). The solution was added to the zeolite sample (350 mg) and the mixture was refluxed at 80 ºC for 5 h. The supported complexes (MOR/**Fe** and MOR-D/**Fe**, respectively for **Fe** heterogenised on commercial and desilicated zeolite) were separated by vacuum filtration using a G4 porous plaque, washed several times with ethanol (Riedel-de-Haën) and dried, firstly overnight at ambient temperature and then at 50 ºC for about 4 h.

2.3. Physicochemical characterization

The structural characterization of the supports (MOR and MOR-D) and complex loaded samples (MOR/**Fe** and MOR-D/**Fe**) was undertaken using X-ray powder difractograms (XRD) that were obtained at room temperature in a Philips PX-1730, using a CuKα radiation as incident beam. Difractograms were obtained by continuous scanning from 5º to 40º 2θ, with a step size of 0.02º 2θ and a time step of 0.4 s.

Far infrared spectra (400-200 cm^{-1}) were recorded on a Vertex 70 spectrophotometer, in CsI pellets.

The metal contents present on the immobilized complexes were analysed by ICP using a ICP-AES Horiba Jobin-Yvon model Ultima equipament at Laboratório de Análises, IST Lisbon, Portugal.

Transmission electron microscopy (TEM) of parent and desilicated support was carried out in a Hitachi, model H-8100 microscope, operating at 200 kV. The images were captured from the thin edges of the particles supported on a carbon grid.

Textural characterization of the supports and complex-loaded samples was made by N_2 adsorption isotherms at -196 ºC in an automatic apparatus Micromeritics ASAP 2010. Before the isotherms acquisition the samples (≈ 50 mg) were outgassed for 2 h at 150 ºC, under vacuum better than 10^{-2} Pa.

2.4. Typical procedure for the catalytic oxidation of cyclohexane and products analysis

The peroxidative oxidation reactions were carried out in Schlenk tubes and under dinitrogen atmosphere as follows: 0.43-6.6 μmol of MOR/**Fe** and MOR-D/**Fe** catalysts and 0.08-1.6 mmol of pyrazine carboxylic acid (Hpca) (Aldrich) or of nitric acid (Fluka) (*i.e.* catalyst:acid molar ratio of 1:100 to 1:2500) were added to 3.00 mL of NCMe (Riedel-de-Haën) with vigorous stirring, whereafter 5.00 mmol of cyclohexane (Aldrich) (0.54 mL) and 10.00 mmol of H_2O_2 in a 30 % H_2O solution (Fluka) (1.02 mL) were added and the reaction solution was stirred for 10 h, at room temperature and normal pressure. For the products analysis, 90 μL of cycloheptanone (Aldrich, internal standard), 10.00 mL of diethyl ether (Riedel-de-Haën, to extract the substrate and the organic products from the reaction mixture) were added. The obtained mixture was stirred during 10 min and then a sample (1 μL) was taken from the organic phase and analysed by gas chromatography (GC) by the internal standard method. Subsequently, an excess of solid triphenylphosphine was added to the final organic phase (to reduce the cyclohexyl hydroperoxide, if formed, to the corresponding alcohol, and hydrogen peroxide to water), and the mixture was analysed again to estimate the amount of cyclohexyl hydroperoxide, following a method developed by Shul'pin [22]. For determination of oxygenate concentrations only data obtained after treatment of the reaction sample with PPh_3 were used. Authentic samples of all oxygenated products were used to attribute the peaks in chromatograms. Blank tests indicate that no oxidation takes place in the absence of the metal catalyst or the oxidant. Eventual leaching of the supported complex was also tested.

GC measurements were carried out using a FISONS Instruments GC 8000 series gas chromatograph with a FID detector and a capillary column (DB-WAX, column length: 30 m; internal diameter: 0.32 mm). The temperature of injection was 240 ºC. The initial temperature was maintained at 100 ºC for 1 min, then raised 10 ºC/min to 180 ºC. Helium was used as the carrier gas. GC-MS analyses were performed using a Perkin Elmer Clarus 600 C instrument. The ionization voltage was 70 eV. Gas chromatography was conducted in the temperature-programming mode, using a SGE BPX5 column (30 m × 0.25 mm × 0.25 µm). Reaction products were identified by comparison of their retention times with known reference compounds, and by comparing their mass spectra to fragmentation patterns obtained from the NIST spectral library stored in the computer software of the mass spectrometer.

3. Results and discussion

The hydrotris(pyrazol-1-yl)methane iron(II) complex $[FeCl_2\{\eta^3\text{-}HC(pz)_3\}]$ (**Fe**, Figure 1) was immobilized in parent (MOR) and desilicated MOR (MOR-D) zeolite supports, using the wet-impregnation method, by the same procedure previously reported by some of us [1h].

- Figure 1 -

3.1. Physicochemical characterisation

The powder XRD patterns of parent (MOR) and desilicated (MOR-D) samples reveal the same long-range crystal ordering, since no important changes in peaks position are registered, as previously discussed [9]. However, in MOR-D the peaks intensity is affected by the alkaline treatment, leading to a decrease of about 25 % of the crystallinity, when compared with the parent zeolite. Upon complex immobilization no significant losses of crystallinity are observed when compared with MOR and MOR-D.

TEM micrographs for MOR and MOR-D samples are displayed in Figure 2. For the parent MOR zeolite (Fig. 2a) the images show the presence of solid dense crystals. Upon desilication (Fig. 2b) the image presents corroded areas at the crystal external surface as well as lighter zones due to the perforation of the crystals as a consequence of the alkaline treatment with relatively high concentrated NaOH solution (0.5 M).

- Figure 2 -

The metal contents present on the immobilized complexes were quantified by ICP in MOR/**Fe** and MOR-D/**Fe** samples and are displayed on Table 1. The loading level of iron immobilization was shown to be 0.28% (wt/wt) of **Fe** on the MOR-D support, corresponding to a catalyst loading of 18.1 mmol per gram of MOR-D, whereas MOR/**Fe** was shown to be 0.40% (wt/wt) of **Fe** on the MOR support, corresponding to a catalyst loading of 25.8 mmol per gram of MOR. The higher content of **Fe** on the parent sample indicates that the interaction of the metal complex with the zeolite is affected by the amount of internal/external surface groups. Indeed, the alkaline treatment performed on zeolites leads to some lost of surface groups, that is, acid sites, along with a decrease in crystallinity, especially when more severe experimental conditions of temperature, time or base concentration are applied, as it was the case of the conditions used to prepare MOR-D. Some of us have already reported [13] the decrease on the acid sites density of desilicated MOR zeolite with the increase of the duration of the treatment, using 0.2 M NaOH solution. Hence, it is predictable that the use of a higher base concentration (0.5 M) leads to a significant loss of acid sites, and decreases the number of possible interactions between the iron complex and the zeolite surface group, leading to a lower amount of Fe immobilized on the support.

The presence of **Fe** loaded on MOR or MOR-D is also detected at the MOR/**Fe** or MOR-D/**Fe** infrared spectra in the 400-200 cm^{-1} range. In fact, both spectra display, compared to MOR (Fig. 3e) or MOR-D (Fig. 3b) spectra, new bands in the 255 - 235 cm^{-1} range (Fig. 3d or Fig. 3a, respectively for MOR/**Fe** or MOR-D/**Fe**) assigned to ν(Fe-Cl) of **Fe** (Fig. 3c), which attest the presence of the Fe complex immobilized on the zeolitic supports.

- Figure 3 -

In Figure 4 the N_2 adsorption-desorption isotherm for MOR, MOR-D and MOR-D/**Fe** are displayed. The curve of the parent structure belongs to type I isotherm in BDDT classification [23], which is in accordance with the microporous nature of MOR zeolite. At relative pressure near 1 a small upwards deviation of the plateau is noticed, pointing out some mesoporosity or external surface, resulting of the aggregation of the small crystallites, typical of commercial zeolites. Upon desilication treatment MOR-D sample exhibits a mix type I+IV isotherm revealing the microporosity of the sample along with a considerable development of mesoporosity, denoted by the increase of the N_2 uptake at relative pressures near unity. After complex immobilization there is a significant reduction of the adsorption capacity of the samples indicating that most probably the complex molecule blocks the entrance of the porous channels.

- Figure 4 -

In order to obtain a quantitative evaluation of porosity evolution the adsorption data were analysed applying the BET equation, to compute the apparent surface area (A_{BET}), and the α_s method (taking as reference the isotherm determined on nonporous silica [24]) to obtain the micropore volume (V_{micro}). These textural parameters along with the external surface area are displayed in Table 1. The desilication conditions used to prepare MOR-D promoted an accentuated development of mesoporosity along with a small decrease of the volume correspondent to micropores. This evolution reveals that the mesoporosity results mainly from the corrosion of the external surface of the crystals, that is, intercrystalline mesoporosity. On the other hand, the decrease in microporous volume also indicates the occurrence of intracristalline mesoporosity. The effect of the complex immobilization on the zeolitic supports is clearly shown as a considerable decrease on all the textural parameters is observed.

Table 1 - Iron content, apparent surface area (A_{BET}), micro (V_{micro}) and total pore volume (V_{total}), and external area (A_{ext}) of the samples.

Sample	%Fe	A_{BET} (m^2/g)	V_{micro} (cm^3/g)	V_{total} (cm^3/g)	V_{meso} (cm^3/g)	A_{ext} (m^2/g)
MOR	-	502	0.20	0.25	0.05	24
MOR/**Fe**	0.40	43	0.01	0.05	0.04	22
MOR-D	-	500	0.17	0.38	0.21	125
MOR-D/**Fe**	0.28	45	0.01	0.10	0.09	25

Considering the predicted dimensions of the iron complex (maximum width ~0.8 nm, by comparison with related η^3-HC(pz)$_3$ Cu complexes) [25] we must consider that the decrease of the micropore volume accessible to N_2 is most likely the result of the blockage of the pore channels characteristic of MOR structure (0.67 x 0.70 nm). In the case of sample MOR-D/**Fe** there is also an important decrease of the mesopore volume, compared to the value presented by the same sample before the immobilization of **Fe** complex (see Table 1) pointing out that at least a fraction of the complex must be located in the intercrystaline mesoporosity created upon desilication. In fact, the mesopore size distribution of the MOR-D reveals the presence of a large fraction of pores with width around 12.5 nm, what is compatible with the predicted dimensions of the complex.

3.2. Catalytic oxidation of cyclohexane

We found that MOR-D/**Fe** exhibits a remarkable catalytic activity (turnover numbers up to *ca*. 2.90 x 10^3, Table 2, entry 8) under mild conditions for the peroxidative oxidation of cyclohexane to the cyclohexanol and cyclohexanone mixture, in a single-pot process (Scheme 1). The catalytic system is based on the above hydrotris(pyrazol-1-yl)methane Fe(II) complex [FeCl$_2${η^3-HC(pz)$_3$}] (**Fe**) supported on desilicated MOR zeolite (MOR-D), hydrogen peroxide (30% aqueous solution) as the oxidizing agent, and acetonitrile as the solvent, in a slightly acidic medium (typically with the presence of pyrazinecarboxylic acid, Hpca), at room temperature and 10 h typical reaction time.

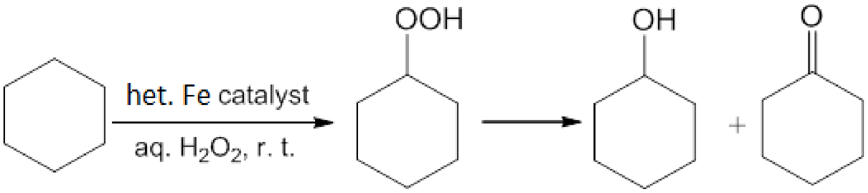

Scheme 1

In order to determine the concentrations of all cyclohexane oxidation products the samples of reaction solutions were analysed twice, that is, before and after treatment with an excess of solid triphenylphosphine (in order to reduce the formed cyclohexyl hydroperoxide to the corresponding alcohol, and hydrogen peroxide to water), following a method developed by Shul'pin [22] and used previously by some of us [2a-d,2f,26]. By applying this method in the present work, we demonstrate that the oxidation of cyclohexane affords predominantly the cyclohexyl hydroperoxide CyOOH as a primary product (Scheme 1) which decomposes to form cyclohexanol and cyclohexanone (a significant increase of the alcohol amount, by *ca*. 40%, with a concomitant decrease of that of the ketone when the final reaction solution, prior to GC analysis, is treated with an excess of PPh_3 was observed).

The achieved TON is remarkably high, much above that found for MOR/**Fe, Fe** [2f] (91 and 232, Table 2, entries 9 and 10, respectively) or for other mononuclear iron complex catalysts [2b,27,28] in homogeneous medium, in spite of the mild conditions, in aqueous acetonitrile at a low temperature with a green oxidant, in the presence of a weak acid.

The yield (up to 37.5% Table 2, entry 8) is also much higher than those observed for MOR/**Fe** (1.8%, Table 2, entry 9), **Fe** (up to 13%) [2f], the related $Li[FeCl_2\{SO_3C(pz)_3\}]$

(up to 24%) [2f], $[Fe\{HOCH_2C(pz)_3\}_2]_2[Fe_2OCl_6](Cl)_2\cdot 4H_2O$ (pz = pyrazolyl; up to 14%) [2b], $[Fe(gma)(PBu_3)]$ ($gmaH_2$ = glyoxal-bis(2-mercaptoanil); up to 8%) [27a], the Co(III)-Fe(III) Schiff base complex $[Co_4Fe_2OSae_8]\cdot 4DMF\cdot H_2O$ (H_2Sae = salicylidene-2-ethanolamine) (up to 26%) [29] and the hexanuclear iron(III) *p*-nitrobenzoate complex $[Fe_6O_3(OH)(p\text{-}NO_2C_6H_4COO)_{11}(dmf)_4]$ (20%) [30]. It is lower than those for Fe(III)-Cr(III) hydroxides [31] (up to 45%) but the latter system requires the use of a strong acid (HNO_3) and leads to a much lower TON value of 30. The combination of such a high yield and TON is rare and indicates an exceptional activity of the catalytic system based on MOR-D/**Fe**. Moreover, the oxidation of cyclohexane with hydrogen peroxide in the presence of decamethylosmocene, $[Os(Me_5C_5)_2]$ and pyridine, also an exceptionally active system [32], needs 24 h to exhibit higher TON values (up to *ca*. 5.1×10^4) and the yields remain low (up to *ca*. 6%). For $[Os_3(CO)_{12}]$ TON values up to 6.0×10^4 (*i.e*. 2.0×10^4 per Os [22b]) are obtained at 60 ºC, whereas in the present work the reactions were performed at room temperature.

A high selectivity towards the formation of cyclohexanol and cyclohexanone is exhibited by our systems, since no traces of by-products were detected by GC-MS analysis of the final reaction mixtures. No alkane oxidation products were obtained in the absence of **Fe** (Table 2, entries 1 and 2) or hydrogen peroxide.

Table 2 - Oxidation of cyclohexane with H_2O_2 (selected data).[a]

Entry	Catalyst	$n(H_2O_2)/n$(catalyst)	n(acid)/n(catalyst)	Time	Total	Total Yield

		x 10^{-3}	x 10^{-3}	h	TON[b]	(%)[c]
1	MOR	20	0	10	-	0.0
2	MOR-D	20	0	10	-	0.0
3[d]	**Fe [**2f]	20	0	6	161	0.8
4	MOR/**Fe**	20	0	10	25	0.5
5	MOR-D/**Fe**	20	0	10	334	4.3
6[e]	MOR	20	1	10	-	0.0
7[e]	MOR-D	20	1	10	-	0.0
8	MOR-D/**Fe**	20	1	10	2.9 x 10^{3}	37.5
9	MOR/**Fe**	20	1	10	91	1.8
10[d, f]	**Fe [**2f]	20	1	6	232	2.3
11[d, f]	**Fe [**2f]	40	1	6	522	2.6
12	MOR-D/**Fe**	20	1	3	575	7.4
13	MOR-D/**Fe**	20	1	6	1.9 x 10^{3}	24.0
14	MOR-D/**Fe**	20	1	12	1.7 x 10^{3}	21.8
15	MOR-D/**Fe**	20	1	17	438	5.6
16	MOR-D/**Fe**	20	1	24	272	3.5
17	MOR-D/**Fe**	3.8	1	10	410	5.3
18	MOR-D/**Fe**	7.5	1	10	672	9.9
19	MOR-D/**Fe**	15	1	10	1.8 x 10^{3}	22.9
20	MOR-D/**Fe**	30	1	10	2.9 x 10^{3}	37.2
21[f]	MOR-D/**Fe**	20	1	10	1.4 x 10^{3}	18.2
22[f]	MOR-D/**Fe**	20	2	10	447	5.7
23[f]	MOR-D/**Fe**	20	0.1	10	609	7.8

24[g]	MOR-D/**Fe**	20	1	10	478	6.1
25[h]	MOR-D/**Fe**	20	1	10	407	5.2
26[i]	MOR-D/**Fe**	20	1	10	371	3.1

[a] Reaction conditions (unless stated otherwise): acetonitrile (3.0 mL), cyclohexane (5.0 mmol), r.t., under dinitrogen; 0.43-6.6 μmol of **Fe**, catalyst:Hpca (molar ratio 1:0 to 1:2.5 x 10^3), H_2O_2 (1:1 to 3 x 10^4:1 molar ratio of oxidant to Fe catalyst). Percentage of yield, TON determined by GC analysis (upon treatment with PPh_3). [b] Total (cyclohexanol + cyclohexanone) turnover number (moles of product per mol of supported catalyst). [c] Molar yield (%) based on substrate, *i.e.* moles of products (cyclohexanol and cyclohexanone) per 100 mol of cyclohexane. [d] The reaction time[2f] leading to the highest yields and TONs for the homogeneous system. [e] Reaction in the presence of Hpca or HNO_3. [f] Reaction in the presence of HNO_3. [g] Reaction with *t*-BuOOH as oxidant. [h] Reaction in water. [i] 2nd run of catalyst used in entry 21.

The high catalytic activity of MOR-D/**Fe** must be related with the textural parameters of the MOR-D support since after immobilization the Fe complex must be located in the intercrystalline mesopores then the accessibility of the reactant molecules is strongly improved leading to higher catalytic activity.

For the purpose of optimization of the catalytic system, the effects of various reaction parameters were examined. Hence, the dependences of the yields of products and the TONs on the oxidant-to-catalyst molar ratio, acid-to-catalyst molar ratio, reaction time and type of acid, oxidant and solvent were investigated for the most active catalyst MOR-D/**Fe**.

3.2.1. Effect of the reaction time

The effect of the reaction time on the TON for MOR-D/**Fe** in the cyclohexane oxidation is depicted on Figure 5. The overall TON (and yield) increases during the first 10 h whereafter a drop is observed, conceivably due to over oxidation. In fact, some products of overoxidation such as 1,4-cyclohexanedione and 1,2-epoxycyclohexane were detected by GC-MS for the conditions of entry 16 in Table 2.

- Figure 5 -

3.2.2. Effect of the amount and type of acid

The presence of Hpca (pyrazinecarboxylic acid) is essential for these reactions to proceed significantly (Table 2, compare entries 5 and 8, Figure 6). The addition of Hpca (up to a Hpca:catalyst molar ratio of 1000:1) leads to a remarkable yield growth for both alcohol and ketone (Figure 6). The co-catalytic effect of Hpca in vanadium-catalysed oxidations was discovered by Shul'pin *et al*. [4f,4h]. Later, a high promoting effect of that heteroaromatic acid on the peroxidative oxidation of alkanes catalyzed by homogeneous iron species [4a,27,33], on the oxyfunctionalization of cyclohexane with dioxygen catalyzed by scorpionate vanadium complexes [2e], as well as by pyrazole-rhenium complexes supported on modified silica gel [1h], was also recognized [34]. The role of Hpca, via coordination of pca (the conjugate base) to iron, conceivably consists in assisting proton-transfer from ligated H_2O_2 to an oxo- or a hydroxo-ligand, thus promoting the formation of hydroperoxyl ($HOO^{\bullet}$) and hydroxyl ($HO^{\bullet}$) radicals, as it was proposed

[4a,4d,4f,4h,22b,33,35] for vanadium catalyst-Hpca-H_2O_2 systems and supported by theoretical calculations [36].

The activity of MOR-D/**Fe** is also promoted by addition of a mineral acid such as HNO_3 (Table 2, entries 21 - 23; Figure 6), as recognized by us for other metal catalysts [2a,2d,2e,2g,26b-d,37], but in a much lower extent.

- Figure 6 -

3.2.3. Effect of the amount and type of oxidant

The effect of the peroxide-to-catalyst molar ratio was investigated and is depicted in Figure 7. The increase of the peroxide amount up to $n(H_2O_2)/n$(MOR-D/**Fe**) molar ratio of $2x10^4$ leads to the maximum products yield of 37.5%. Further increase of the oxidant amount does not result in a higher product yield, on account of overoxidation at higher H_2O_2 amounts (1,4-cyclohexanedione was detected by GC-MS for the conditions of entry 20 in Table 2).

- Figure 7 -

Hydrogen peroxide behaves as a more effective oxidizing agent than *tert*-butyl hydroperoxide (70%) (Table 2, entries 8 and 24, respectively), conceivably due to the bulky character of the *t*-butyl group in the latter (resulting in a higher difficulty to reach the supported iron complex).

3.2.4. Effect of the type of solvent

Acetonitrile was chosen as the typical solvent for our systems due to its high resistance to oxidizing agents and also in view of the good solubility of the substrate. It has also been used [1h,2] in other cases as the most appropriate solvent for cyclohexane oxidations, namely with [$FeCl_2$\{η^3-HC$(pz)_3$\}] in homogeneous media [2f]. The attempt to replace acetonitrile by a greener solvent, such as water, results in a drastic decrease of activity (from 37.5% to 5.2%, Table 2, entries 8 and 25, respectively).

3.2.5. Catalyst recycling

In order to investigate the recyclability of the MOR-D/**Fe** system, on completion of a stage, the products were analysed as usually and the supported catalyst was recovered by filtration from the reaction mixture, washed several times with acetonitrile and dried overnight at 50 º C. The subsequent cycle was initiated upon addition of new standard portions of all other reagents; MOR-D/**Fe** exhibited 54% of its initial activity (Table 2, entry 26), while maintaining the selectivity. This recycling possibility was not possible [2f] for **Fe** for the peroxidative oxidation of cyclohexane.

Moreover, the amount of Fe on MOR-D/**Fe** after the first catalytic run was quantified. A decrease of about half of the initial content was determined (0.28% to 0.12% of supported Fe on MOR-D), which indicates the occurrence of lixiviation phenomena during the catalytic reaction or catalyst recovery and that the type of interaction between **Fe** and the support is weak (probably of the electrostatic type) [38].

Surprisingly, only traces of cyclohexanol and cyclohexanone were found in a run performed with the filtered solution from a first run (Table 2, entry 22) taken to dryness, to which new standard portions of all other reagents were added. This suggests the formation of new inactive species from **Fe** upon the release from the zeolitic support.

4. Conclusions

This study has contributed towards the development of the still unexplored application of transition metal complexes supported on desilicated zeolites as catalyst and/or catalyst precursor for the oxidation of cyclohexane to the cyclohexanol and cyclohexanone mixture, under mild conditions and with an environmentally friendly oxidant (H_2O_2).

The generation of mesoporosity in commercial MOR by desilication revealed to be a good strategy to improve the immobilization of the $[FeCl_2\{\eta^3\text{-}HC(pz)_3\}]$ complex on the zeolitic support and appears to be crucial for its catalytic activity. In fact, the heterogeneous MOR-D/**Fe** system is notably more efficient (much higher TON and yield values and lower loading of oxidant) than the homogeneous C-scorpionate iron(II) complex.

The heterogeneous system also offered practical advantages of recycling (by the facile separation from products), allowing successive cycles, although with a considerable loss of activity, mainly due to lixiviation (54 % from the 1st to the 2nd cycle), an aspect which deserves to be further addressed.

Acknowledgments

This work has been partially supported by the Fundação para a Ciência e a Tecnologia (FCT), Portugal, and projects PTDC/QUI-QUI/102150/2008, PTDC/EQU-EQU/122025-2010 and PEst-OE/QUI/UI0100/2011, PEst-OE/QUI/UI0612/2011 (CQB) and PEst-OE/EQB/UI0702/2011 (CIEQB).

References

---

[1] a) C. Pettinari, Scorpionates II: Chelating Borate Ligands, Imperial College Press, London, 2008; b) C. Pettinari, R. Pettinari, Coord. Chem. Rev. 249 (2005) 525-543; c) C. Pettinari, C. Santini, Polypyrazolylborate and Scorpionate Ligands, in: J.A. McCleverty, T.J. Meyer (Ed.), Comprehensive Coordination Chemistry II: From Biology to Nanotechnology, vol. 1, Elsevier Pergamon (APS), Amsterdam 2003, pp. 159; d) R. Wanke, M.F.C. Guedes da Silva, S. Lancianesi, T.F.S. Silva, L.M.D.R.S. Martins, C. Pettinari, A.J.L. Pombeiro, Inorg. Chem. 49 (2010) 7941-7952; e) Pettinari, F. Marchetti, G. Lupidi, L. Quassinti, M. Bramucci, D. Petrelli, L.A. Vitali, M.F.C. Guedes da Silva, L.M.D.R.S. Martins, P. Smolenski, A.J.L. Pombeiro, Inorg. Chem. 50 (2011) 11173-11183; f) T.F.S. Silva, L.M.D.R.S. Martins, M.F. Guedes da Silva, A.R. Fernandes, A. Silva, P.M. Borralho, S. Santos, C.M.P. Rodrigues, A.J.L. Pombeiro, Dalton Trans. 41 (2012) 12888-12897; g) E.C.B. Alegria, L.M.D.R.S. Martins, M.V. Kirillova, A.J.L. Pombeiro, Appl. Cat.

A: General 443-444 (2012) 27-32; h) G.S. Mishra, E.C.B.A. Alegria, L.M.D.R.S. Martins, J.J.R. Fraústo da Silva, A.J.L. Pombeiro, J. Mol. Cat. A: Chem 285 (2008) 92-100; i) L.M.D.R.S. Martins, E.C.B.A. Alegria, P. Smoleński, M.L. Kuznetsov, A.J.L. Pombeiro, Inorg. Chem. 52 (2013) 4534-4546.

[2] a) T.F.S. Silva, T.C.O. Mac Leod, L.M.D.R.S. Martins, M.F. Guedes da Silva, A.J.L. Pombeiro, J. Mol. Cat. A: Chem. 367 (2013) 52-60; b) T.F.S. Silva, M.F.C.G. Silva, G.S. Mishra, L.M.D.R.S. Martins, A.J.L. Pombeiro, J. Organomet. Chem. 696 (2011) 1310-1318; c) T.F.S. Silva, K.V. Luzyanin, M.V. Kirillova, M.F.C.G. Silva, L.M.D.R.S. Martins, A.J.L. Pombeiro, Adv. Synth. Cat. 352 (2010), 171-187; d) T.F.S. Silva, G.S. Mishra, M.F.G. Silva, R. Wanke, L.M.D.R.S. Martins, A.J.L. Pombeiro, Dalton Trans. (2009) 9207-9215; e) G.S. Mishra, T.F.S. Silva, L.M.D.R.S. Martins, A.J.L. Pombeiro, Pure Appl. Chem. 81 (2009) 1217-1227; f) T.F.S. Silva, E.C.B.A. Alegria, L.M.D.R.S. Martins, A.J.L. Pombeiro, Adv., Synth. Cat. 350 (2008) 706-716; g) E.C.B.A. Alegria, M.V. Kirillova, L.M.D.R.S. Martins, A.J.L. Pombeiro, Appl. Catal. A: Gen., 317 (2007) 43-52.

[3] a) G.B. Shul'pin, in: M. Beller, C. Bolm (Ed.), 2nd ed., Transition Metals for Organic Synthesis, vol. 2. Wiley-VCR, New York, 2004, pp. 215; b) A.E. Shilov, G.B. Shul´pin, Activation and Catalytic Reactions of Saturated Hydrocarbons in the Presence of Metal Complexes, Kluwer Academic Publisher, Dordrecht, 2000; c) E.G. Derouane, V. Parmon, F. Lemos, F. Ramôa Ribeiro (Ed.), Sustainable strategies for the upgrading of natural gas: Fundamentals, challenges and opportunities. NATO ASI Series, vol. 191, Springer, Dordrecht, 2005; d) E.G. Derouane, J. Haber, F. Lemos, F. Ramôa Ribeiro, M. Guinet (Ed.), Catalytic Activation and Functionalization of Light Alkanes, NATO ASI Series, vol.

44, Kluwer Academic Publisher, Dordrecht, 1998; e) R.H. Crabtree, J. Organomet. Chem. 689 (2004), 4083-4091; f) R.H. Crabtree, J. Chem. Soc., Dalton Trans. (2001) 2437-2450; g) Handbook of Green Chemistry and Technology, Ed.: D.J. Macquarrie, J. Clark, Blackwell Publishing Technology & Industrial Arts, 2002; h) Ullmann's Encyclopedia of Industrial Chemistry, 6th ed., Wiley-VCH, Weinheim, 2002; i) W. Weissermel, H.J. Horpe, Industrial Org. Chem., 2nd ed., VCH Press, Weinheim, 1993; j) R.A. Sheldon, I.W.C.E. Arends, U. Hanefeld, Green Chemistry & Catalysis, Wiley-VCH, Weinheim, 2007.

[4] a) G.B. Shul'pin, G.V. Nizova, Y.N. Kozlov, L.G. Cuervo, G. Süss-Fink, Adv. Synth. Catal. 346 (2004) 317-332; b) U. Schuchardt, D. Cardoso, R. Sercheli, R. Pereira, R.S. da Cruz, M.C. Guerreiro, D. Mandelli, E.V. Spinacé, E.L. Pires, J. Appl. Catal. A: Gen. 211 (2001) 1-17; c) U. Schuchardt, D. Mandelli, G.B. Shul'pin, Tetrahedron Lett. 37 (1996) 6487-6490; d) G.B. Shul'pin, J. Mol. Cat. A: Chem. 189 (2002) 39-66; e) G.B. Shul'pin, G.V. Nizova, React. Kinet. Catal. Lett. 48 (1992) 333-338; f) G.B. Shul'pin, D. Attanasio, L. Suber, J. Catal. 142 (1993) 147-152; g) K.S. Anisia, A. Kumar, Appl. Catal. A: Gen. 273 (2004), 193-200; h) G.B. Shul'pin, Y.N. Kozlov, G.V. Nizova, G. Süss-Fink, S. Stanislas, A. Kitaygorodskiy, V.S. Kulikova, J. Chem. Soc., Perkin Trans. 2 (2001) 1351-1371.

[5] C.E. Song, S. Lee, Chem. Rev. 102 (2002) 3495-3524.

[6] Q.-H. Fan, Y.-M. Li, A.S.C. Chan, Chem. Rev. 102 (2002) 3385-3466.

[7] H.W. Xing, X.W. Li, G.L. Tian, Y.H. Ye, Tetrahedron 56 (2000), 3517-3522.

[8] R. Le Van Mao, S. Xiao, A. Ramsaran, J. Yaot, J. Mat. Chem. 4 (1994) 605-610.

---

[9] V. Paixão, A.P. Carvalho, J. Rocha, A. Fernandes, A. Martins, Microporous Mesoporous Mat. 131 (2010) 350-357.

[10] J. Kim, M. Choi, R. Ryoo, J. Catal. 269 (2010) 219-228.

[11] J. Pérez-Ramírez, S. Abelló, A. Bonilla, J.C. Groen, Adv. Funct. Mater. 19 (2009) 164-172.

[12] A. Bonilla, D. Baudouin, J. Pérez-Ramírez, J. Catal. 265 (2009) 170-180.

[13] V. Paixão, R. Monteiro, M. Andrade, A. Fernandes, J. Rocha, A.P. Carvalho, A. Martins, Appl. Catal. A: Gen. 402 (2011) 59-68.

[14] J.C. Groen, T. Sano, J.A. Moulijn, J. Pérez-Ramírez, J. Catal. 251 (2007) 21-27.

[15] M. Akgül, A. Karabakan, Microporous Mesoporous Mat. 145 (2011) 157-164.

[16] S. Mitchell, J. Pérez-Ramirez, Catal. Today 168 (2011) 28-37.

[17] X.-F. Guo, G.-J. Kim, Top. Catal. 53 (2010) 510-516.

[18] M.-J. Jin, A. Taher, Hee-Jae Kang, M. Choi, R. Ryoo, Green Chem. 11 (2009) 309-313.

[19] F. Alirio, M. Guisnet in M. Guisnet, J.-P. Gilson (Ed.) Zeolites for Cleaner Technologies, Catalytic Science Series, Vol. 3, Imperial College Press, Singapore, 2002 (Ch. 4).

[20] M.M. Otten, M.J. Clayton, H.H. Lamb, J. Catal. 149 (1994), 211-222.

[21] D.L. Reger, T.C. Grattan, K.J. Brown, C.A. Little, J.J.S. Lamba, A.L. Rheingold, R.D. Sommer, J. Organom. Chem. 607 (2000) 120-128.

[22] a) G.B. Shul'pin, J. Mol. Cat. A: Chem. 189 (2002) 39-66; b) G.B. Shul’pin, C. R. Chimie, 6 (2003) 163–178; c) G.B. Shul’pin, Y.N. Kozlov, L.S. Shul’pina, A.R. Kudinov,

---

D. Mandelli, Inorg. Chem. 48 (2009) 10480–10482; d) G.B. Shul'pin, Y.N. Kozlov, L.S. Shul'pina, P.V. Petrovskiy, Appl. Organomet. Chem. 24 (2010) 464–472. e) G.B. Shul'pin, Mini-Rev Org. chem. 6 (2009) 95-104.

[23] B. Brunauer, L.S. Deming, W.E. Deming, E. Teller, J. Am. Chem. Soc. 62 (1940) 1723-1732.

[24] S.J. Greg, K.S.W. Sing, Adsorption, Surface Area and Porosity, 2nd ed. Academic Press, London, 1982.

[25] T.F.S. Silva, L.M.D.R.S. Martins, M.F.C. Guedes da Silva, A.J.L. Pombeiro, Acta Cryst., E63 (2007) m1979.

[26] a) M. Sutradhar, M.V. Kirillova, M.F.C. Guedes da Silva, L.M.D.R.S. Martins, A.J.L. Pombeiro, Inorg. Chem. 51 (2012) 11229−11231. b) C. Di Nicola, F. Garau, Y.Y. Karabach, L.M.D.R.S. Martins, M. Monari, L. Pandolfo, C. Pettinari, A.J.L. Pombeiro, Eur. J. Inorg. Chem. (2009) 666-676; c) S. Contaldi, C. Di Nicola, F. Garau, Y.Y. Karabach, L.M.D.R.S. Martins, M. Monari, L. Pandolfo, C. Pettinari, A.J.L. Pombeiro, Dalton Trans. (2009) 4928-4941; d) M.N. Kopylovich, A.C.C. Nunes, K.T. Mahmudov, M. Haukka, T.C.O. Mac Leod, L.M.D.R.S. Martins, M.L. Kuznetsov, A.J.L. Pombeiro, Dalton Trans. 40 (2011) 2822-2836;

[27] a) R.R. Fernandes, M.V. Kirillova, J.A.L. da Silva, J.J.R. Fraústo da Silva, A.J.L. Pombeiro, Appl. Cat. A. General 353 (2009) 107-112; b) R.R. Fernandes, J. Lasri, M.F.C. Guedes da Silva, J.A.L. Silva, J.J.R. Fraústo da Silva, A.J.L. Pombeiro, J. Mol. Cat. A: Chem. 351 (2011) 100-111; c) R.R. Fernandes, J. Lasri, A.M. Kirillov, M.F.C. Guedes da

Silva, J.A.L. Silva, J.J.R. Fraústo da Silva, A.J.L. Pombeiro, Eur. J. Inorg. Chem. (2011) 3781–3790.

[28] M.N. Kopylovich, T.C. Mac Leod, M. Haukka, G.I. Amanullayeva, K.T. Mahmudov, A.J.L. Pombeiro, J. Inorg. Biochem. 115 (2012) 72-77.

[29] D.S. Nesterov, E.N. Chygorin, V.N. Kokozay, V.V. Bon, R. Boca, Y.N. Kozlov, L.S. Shul'pina, J. Jezierska, A. Ozarowski, A.J.L. Pombeiro, G.B. Shul'pin, Inorg. Chem. 51 (2012) 9110-9122.

[30] G. Trettenhahn, M. Nagl, N. Neuwirth, V.B. Arion, W. Jary, P. Pochlauer, W. Schmid, Angew. Chem. Int. Ed. 45 (2006) 2794-2798.

[31] M.N. Kopylovich, A.M. Kirillov, A.K. Baev, A.J.L. Pombeiro, J. Mol. Catal. A: Chem. 206 (2003) 163–178.

[32] G.B. Shul'pin, M.V. Kirillova, Y.N. Kozlov, L.S. Shul'pina, A.R. Kudinov, A.J.L. Pombeiro, J. Cat. 277 (2011) 164-172.

[33] G.V. Nizova, B. Krebs, G. Suss-Fink, S. Schindler, L. Westerheide, L.G. Cuervo, G.B. Shul'pin, Tetrahedron 58 (2002) 9231-9237.

[34] A.M. Kirillov, G.B. Shul'pin, Coord. Chem. Rev. 257 (2013) 732-754.

[35] a) N.Y. Kozlov, B.V. Romakh, A. Kitaygorodskiy, P. Buglyó, G. Suss-Fink, G.B. Shul'pin, J. Phys.Chem. A 111 (2007) 7736-7752; b) M. V. Kirillova, M.L. Kuznetsov, V.B. Romakh, L.S. Shul'pina, J.J.R. Fraústo da Silva, A.J.L. Pombeiro, G.B. Shul'pin, J. Cat. 267 (2009) 140-157.

---

[36] a) R.Z. Khaliullin, A.T. Bell, M. Head-Gordon, J. Phys.Chem. B 109 (2005) 17984-17992; b) M.V. Kirillova, M.L. Kuznetsov, Y.N. Kozlov, L.S. Shul'pina, A. Kitaygordskiy, A.J.L. Pombeiro, G.B. Shul'pin, ACS Cat. 1 (2011) 1511-1520.

[37] a) D.S. Nesterov, V.N. Kokozay, V.V. Dyakonenko, O.V. Shishkin, J. Jezierska, A. Ozarowski, A.M. Kirillov, M.N. Kopylovich, A.J.L. Pombeiro, Chem. Commun. (2006) 4605-4607; b) A.M. Kirillov, M.N. Kopylovich, M.V. Kirillova, M. Haukka, M.F.C.G. da Silva, A.J.L. Pombeiro, Angew. Chem. Int. Ed. 44 (2005) 4345-4349.

[38] J.L. Figueiredo, M.M. Pereira, J. Faria (Ed.), Catalysis from Theory to Application, An Integrated Course, Imprensa da Universidade de Coimbra (2008) p. 213.

Figure captions

Figure 1 - Catalyst precursor for cyclohexane oxidation used in this study: $[FeCl_2\{\eta^3\text{-}HC(pz)_3\}]$ (**Fe**).

Figure 2 - TEM images of (a) parent (MOR) and (b) desilicated MOR (MOR-D) zeolites.

Figure 3 - Infrared spectra in the 320-200 cm^{-1} range of (a) MOR-D/**Fe**, (b) MOR-D, (c) **Fe**, (d) MOR/**Fe** and (e) MOR.

Figure 4 - Nitrogen adsorption–desorption isotherms at −196 ◦C on MOR (□), MOR-D (Δ) and MOR-D/**Fe** (○) samples (closed symbols are desorption points).

Figure 5 - Dependence of the overall (cyclohexanol + cyclohexanone) turnover number (TON, moles of products per mol of supported catalyst MOR-D/**Fe**) on the reaction time. Reaction conditions: r.t., CH_3CN (3.0 mL), cyclohexane (5.0 mmol), $n(H_2O_2)/n$(MOR-D/**Fe)** (2 x10^4), n(acid)/n(MOR-D/**Fe**) (1 x 10^3).

Figure 6 - Effects of the Hpca amount (▲) and of the HNO_3 amount (■) on the overall yield (mol%, based on substrate) of the products of cyclohexane oxidation. Reaction conditions: $n(H_2O_2)/n$(MOR-D/**Fe**) (2 x 10^4), CH_3CN (3.0 mL), cyclohexane (5.0 mmol), 10 h, r.t..

Figure 7 - Dependence of the overall (cyclohexanol + cyclohexanone) yield (mol%, based on substrate) on the amount of oxidant (H_2O_2, molar ratio relatively to MOR-D/**Fe**) in the oxidation of cyclohexane. Reaction conditions: $n(H_2O_2)/n$(MOR-D/**Fe)** (0 – 3 x 10^4), CH_3CN (3.0 mL), cyclohexane (5.0 mmol), n(Hpca)/n(MOR-D/**Fe)** (1 x 10^3), 10 h, r.t..

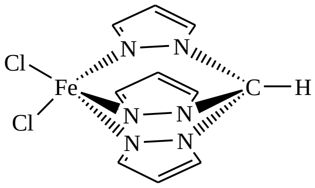

Figure 1

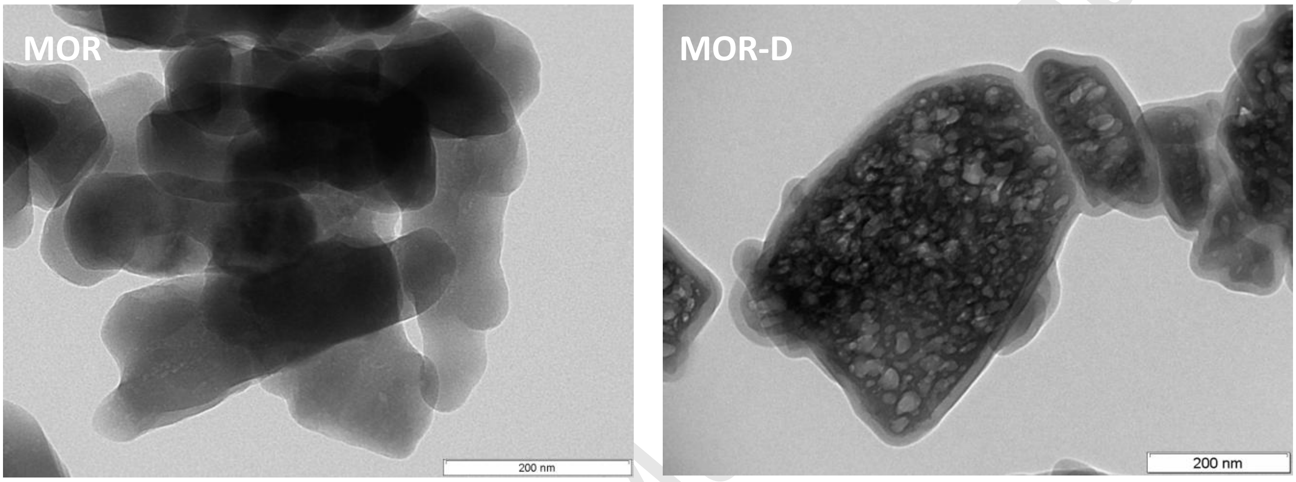

(a)

(b)

Figure 2

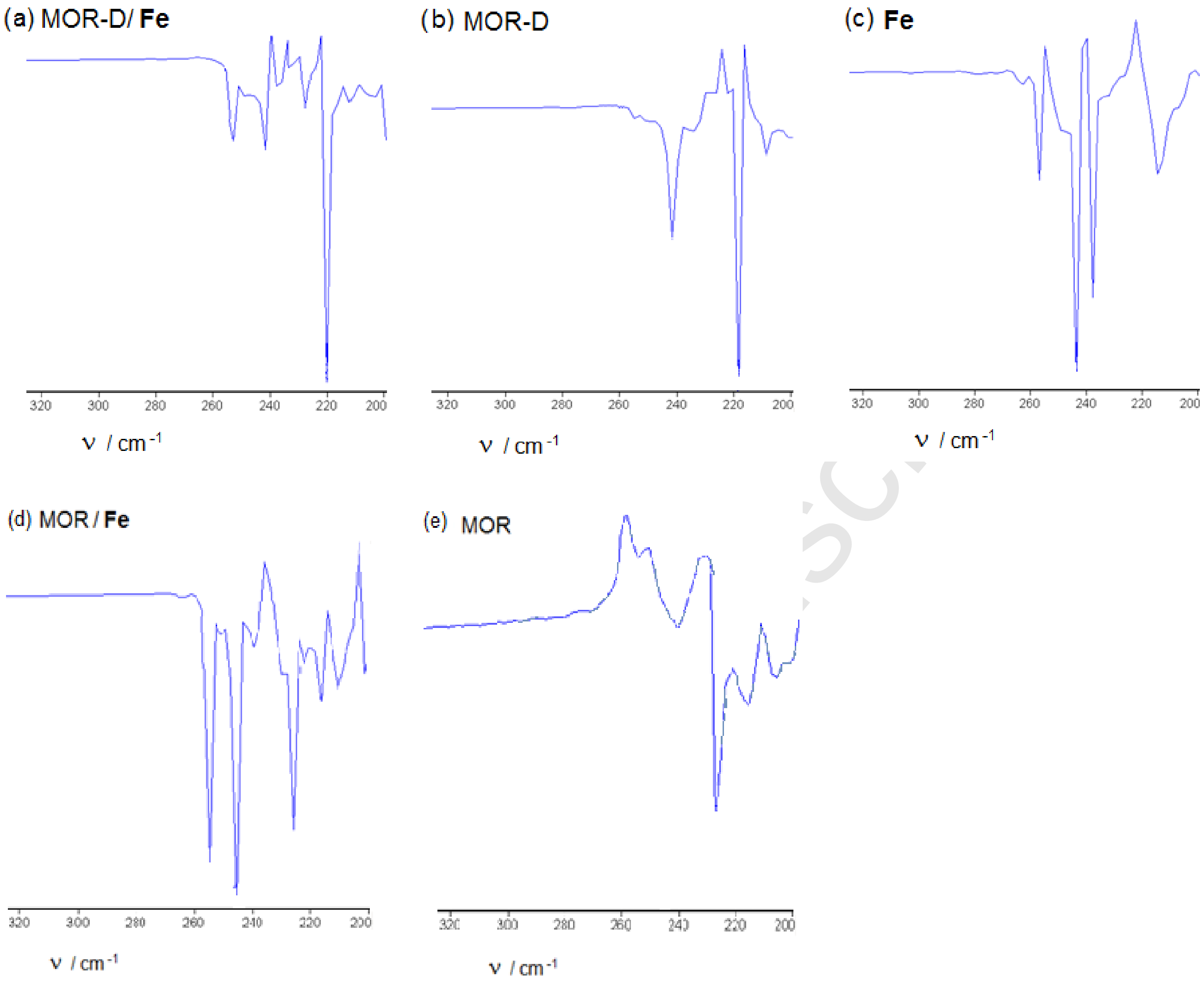
(a) MOR-D/ **Fe**
320 300 280 260 240 220 200
ν / cm^{-1}
(b) MOR-D
320 300 280 260 240 220 200
ν / cm^{-1}
(c) **Fe**
320 300 280 260 240 220 200
ν / cm^{-1}
(d) MOR / **Fe**
320 300 280 260 240 220 200
ν / cm^{-1}
(e) MOR
320 300 280 260 240 220 200
ν / cm^{-1}

Figure 3

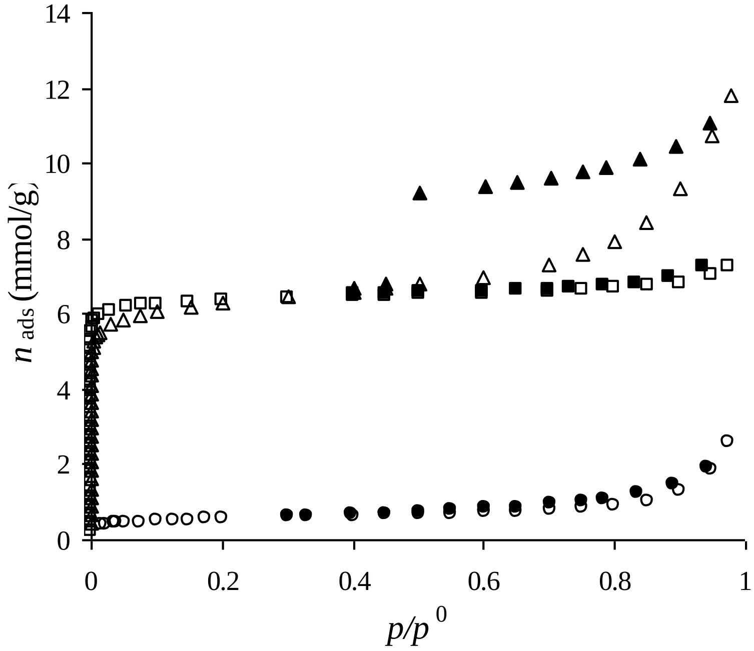

Figure 4

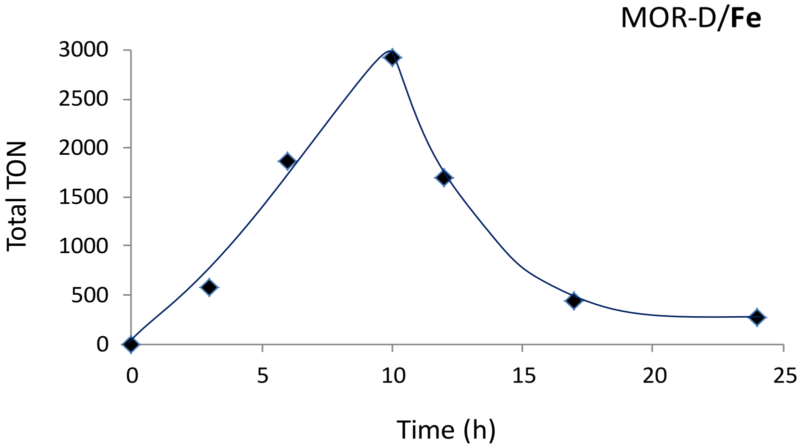

Figure 5

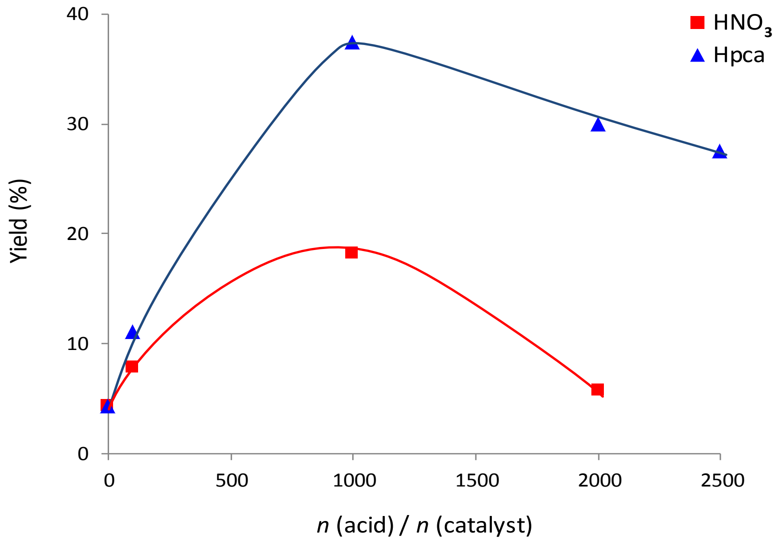

Figure 6

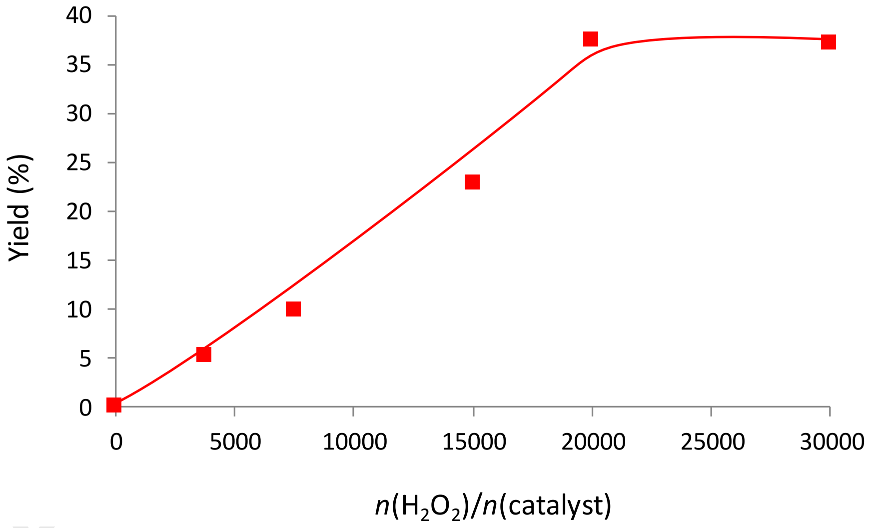

Figure 7